crystals

MDPI

Article

The Influence of CaF_2 Doping on the Sintering Behavior and Microwave Dielectric Properties of $CaO-B_2O_3-SiO_2$ Glass-Ceramics for LTCC Applications

Chao Dong [1,2], Hua Wang [1,*], Tingnan Yan [2], Jianwei Zhao [2], Jiwen Xu [1,*] and Dawei Wang [3,*]

[1] School of Materials Science and Engineering, Guilin University of Electronic Technology, Guilin 541004, China
[2] Shenzhen Institute of Advanced Electronic Materials, Shenzhen Institute of Advanced Technology, Chinese Academy of Sciences, Shenzhen 518055, China
[3] School of Instrumentation Science and Engineering, Harbin Institute of Technology, Harbin 150080, China
* Correspondence: wh65@guet.edu.cn (H.W.); csuxjw@126.com (J.X.); wangdawei102@gmail.com (D.W.)

Abstract: With the rapid development of microelectronic information technology, microelectronic packaging has higher requirements in terms of integration density, signal transmission speed, and passive component integration. Low temperature co-fired ceramics (LTCC) exhibit excellent dielectric properties and low temperature sintering properties, which meets the above-mentioned requirements. This work investigates the effects of CaF_2 doping (0–16 mol%) on the glass structure, sintering behavior, crystallization, microstructure, and microwave dielectric properties of the $CaO-B_2O_3-SiO_2$ (CBS) glass-ceramic system. Glass-ceramics were prepared using the conventional melting and quenching method. The physical and chemical properties of the glass-ceramics were analyzed using various techniques including TMA, SDT, FTIR, XRD, SEM, and a network analyzer. The results indicate that CaF_2 doping can effectively reduce the sintering temperature and softening temperature of CBS ceramics. It also substantially improves the densification, dielectric, and mechanical properties. The appropriate amount of CaF_2-doped CBS glass-ceramics can be sintered below 800 °C with a low dielectric constant and loss at high frequency ($\varepsilon_r < 6$, $\tan\delta < 0.02$ @ 10~13 GHz). Specifically, 8 mol% CaF_2 doped CBS glass-ceramics sintered at 790 °C exhibit excellent microwave dielectric and thermal properties, with $\varepsilon_r \sim 5.92$ @ 11.4 GHz, $\tan\delta \sim 1.59 \times 10^{-3}$, CTE ~ 7.76×10^{-6}/°C, $\lambda \sim 2.17$ W/(m·k), which are attractive for LTCC applications.

Keywords: LTCC; $CaO-B_2O_3-SiO_2$; glass-ceramics; microwave dielectric properties

Citation: Dong, C.; Wang, H.; Yan, T.; Zhao, J.; Xu, J.; Wang, D. The Influence of CaF_2 Doping on the Sintering Behavior and Microwave Dielectric Properties of $CaO-B_2O_3-SiO_2$ Glass-Ceramics for LTCC Applications. *Crystals* **2023**, *13*, 748. https://doi.org/10.3390/cryst13050748

Academic Editor: Maria Gazda

Received: 16 March 2023
Revised: 25 April 2023
Accepted: 26 April 2023
Published: 30 April 2023

1. Introduction

In recent years, the development of modern microelectronics technology has led to the miniaturization, integration, and high efficiency of electronic equipment. With the trend towards miniaturization and high-density assembly of electronic components, substrate materials must have lower sintering temperatures and better dielectric properties. Low temperature co-fired ceramics (LTCC) technology is a new material technology that was first developed by Hughes in 1982 [1]. LTCC technology utilizes low temperature sintered ceramic powder to create a precise and dense raw porcelain belt. This raw porcelain belt is then processed using laser punching, microhole grouting, precision conductor slurry printing, and other processes to create the required circuit graphics. Multiple passive components, such as capacitance, resistance, filter, impedance converter, coupler, are then buried in a multilayer ceramic substrate. The substrate is stacked together, and the internal and external electrodes can use metals such as Au, Ag, and Cu. The entire structure is then sintered at below 900 °C, resulting in a high-density circuit [2]. This technology can also be used to create a 3D circuit substrate with built-in passive components. IC and active devices can be attached to the surface of the substrate, creating a passive/active integrated functional module. The circuit can be further miniaturized and densely packed.

LTCC technology has many technological advantages in the field of high-frequency communication, especially in 5G communication [3]. The technology has excellent electrical, thermal, mechanical, and processing properties and can meet the technical requirements of low-frequency, digital, radio frequency, and microwave device assembly. It is widely used in electronic packaging and has become the focus of research for domestic scientific research institutes in recent years [4]. Among numerous LTCC systems, the CaO-B_2O_3-SiO_2 (CBS) glass-ceramic system, with wollastonite as the main crystalline phase, is highly regarded due to its low dielectric constant ($\varepsilon_r < 6$), low loss ($\tan\delta < 2 \times 10^{-3}$), and similar coefficient of thermal expansion (CTE) to silicon chips ($3.5 \times 10^{-6}/°C$) [5]. CBS glass-ceramics can be fired at low temperature (<900 °C) using Cu, Ag, and other low melting point and high conductivity electrode materials, which greatly reduces the manufacturing cost and is suitable for mass production. Although CBS systems have been commercially used, there are still some obvious problems, such as high sintering temperature and a low sintering densification degree. A great number of works have reported on the influence of doping the CBS glass-ceramics with various additives to improve the comprehensive properties of the CBS system. For instance, Lin et al. [6] have reported about CBS glass-ceramics doped with Ta_2O_5; their results indicated that the crystallization activation energy (Ea) and the glass stability factor (ΔT) of the $CaSiO_3$ phase increased, and the $CaSiO_3$ phase was inhibited by the addition of Ta_2O_5. Liu et al. [7] have reported that the addition of Al_2O_3 could improve the sintering characterization and dielectric properties of CBS ceramics. He et al. [8] have reported that doping CBS glass-ceramics with 2 wt% of TiO_2 reduced the sintering temperature of the CBS glass-ceramics and promoted the recrystallization of the β-$CaSiO_3$ crystalline phase. Zhu et al. [9] have reported the influence of BaO content on the crystallization behavior of the BaO-CaO-B_2O_3-SiO_2 glass-ceramics system. Their results showed that the BaO content raised the resistance of the glass against crystallization and favored the transformation of β-$CaSiO_3$ and α-$CaSiO_3$ phases. Xiang et al. [10] have reported the influence of La_2O_3 addition on the phase transformation and microwave dielectric properties of CBS ceramics, which showed that as the content of La_2O_3 increased, the crystallization tendency of CaB_2O_4 was suppressed. Han et al. [11] investigated the effects of CeO_2 contents on the structure, crystallization behavior, and dielectric properties of CBS glass composition, showing that when the addition of CeO_2 was more than 1 mol%, the $CeO_{1.695}$ phase occurred, and changed to be the main crystalline phase when the content of CeO_2 increased to 10 mol%. He et al. [12] investigated the influence of ZrO_2 content on crystallization, densification, and dielectric performance of CBS glass-ceramics, and their results showed that ZrO_2 content promoted the precipitation of the wollastonite crystal phase. Yang et al. [13] found that additives Na_2O and K_2O could significantly improve the sintering characteristics and dielectric properties. In addition, Zhu et al. [14] demonstrated that an addition of 3 wt% LiF significantly reduced the sintering temperature of CBS glass-ceramics to 790 °C, as well as improved the dielectric properties and bending strength. Fluorides often have low electronic polarizabilities and ionic oscillator strengths per volume. Pei et al. [15] have reported the effects of CaF_2 on the sintering and crystallization of CaO-MgO-Al_2O_3-SiO_2 glass-ceramics. Their results showed that the glass transition temperature, crystallization peak temperature and the activation energy for crystallization decreased with the addition of CaF_2. Wei et al. [16] have reported about the crystallization kinetics of CaF_2 doped wollastonite glass ceramics. Their results showed that the crystallization activation energy of wollastonite glass ceramics can be reduced by adding CaF_2, indicating that CaF_2 was helpful to the viscous flow of the glass phase and increased its ability to promote glass crystallization. Wei et al. [17] have further reported the reaction crystallization of sodium-calcium glass powders with different amounts of CaF_2, which showed that the sintered glass ceramics were formed by reaction crystallization at 850 °C with 6% CaF_2. With the increase in CaF_2 content, the porosity, volume density, and flexural strength of the sintered ceramics increased gradually. Zhao et al. [18] have reported the effects of CaF_2 addition on the crystallization process and material properties of glass-ceramics. Their results showed that adding the proper amount of CaF_2 could

reduce the crystallization temperature and increase crystallization. Wei et al. [19] have reported the effects of adding fluoride on properties of wollastonite glass ceramics, which showed that the main crystalline phase of glass-ceramics prepared by adding MgF_2, BaF_2, or compound fluoride was wollastonite. Qin et al. [20] investigated the crystal structure, lattice vibration, and microwave dielectric properties of $3CaO\text{-}2SiO_2\text{-}xCaF_2$ ceramics. The results showed that with the increase of CaF_2, the crystal structure of $3CaO\text{-}2SiO_2\text{-}xCaF_2$ ceramics transferred from rankinite ($Ca_3Si_2O_7$) to cuspidine ($Ca_4Si_2O_7F_2$), with reduced permittivity and quality factor. However, the effect of CaF_2 on the crystallization behavior and microwave dielectric properties of the CBS glass-ceramics has few reports so far. Therefore, in this work, the effects of CaF_2 doping on the glass structure, sintering behavior, crystallization, microstructure, and microwave dielectric properties of CBS glass-ceramic systems have been investigated in detail.

2. Materials and Methods

The $CaO\text{-}B_2O_3\text{-}SiO_2\text{-}CaF_2$ (CBSF) glass-ceramics were synthesized via the conventional melting and quenching method, in which the starting materials included analytical reagent-grade CaO, SiO_2, B_2O_3, and CaF_2. In accordance with previous research [21], a basic glass composition was selected with a CaO/SiO_2 ratio of 1 and a B_2O_3 content of 7.5 mol%. Various amounts of CaF_2 (0–16 mol%) were added to the base composition to obtain glass-ceramic samples denoted as CBSF0, CBSF1, CBSF2, CBSF3, and CBSF4, respectively. Stoichiometric molar ratios of the raw materials were followed as per Table 1. The raw materials were weighed accurately and dry-milled using zirconia balls for 12 h, followed by sieving. The mixed powders were then melted at 1500 °C for 2 h in a platinum crucible to obtain glass frits. To prevent crystallization, the melt was rapidly quenched into deionized water. The glass frits were then dried and ball-milled with agate balls and ethyl alcohol for 8 h to obtain glass slurry with a particle size of 2~3 μm. Subsequently, the slurry was dried at 80 °C to obtain dried CBS fine glass powder, which was mixed with polyvinyl acetate (PVA) solution as a binder for manual granulation.

Table 1. The ingredients of $CaO\text{-}B_2O_3\text{-}SiO_2\text{-}CaF_2$ glass (Ts: softening temperature).

Sample	CaO (mol%)	B_2O_3 (mol%)	SiO_2 (mol%)	CaF_2 (mol%)	Ts (°C)
CBSF0	46.25	7.5	46.25	0	738
CBSF1	44.25	7.5	44.25	4	712
CBSF2	42.25	7.5	42.25	8	692
CBSF3	40.25	7.5	40.25	12	673
CBSF4	38.25	7.5	38.25	16	662

The granulated powder was poured into the mold and pressed into 13 mm × 5 mm, 6 mm × 5 mm cylindrical, and 10 × 1.5 mm pellets by an automatic uniaxial compressing machine (ZYP-20TS, Xinnuo Instruments, Shanghai, China) under 156 MPa, 30 MPa, and 100 MPa, separately. The green samples were heated at 550 °C for 5 h to remove the binder and then sintered at various temperatures (750, 775, 780, 790, 800, 825, and 850 °C) for 30 min with a heating rate of 5 °C /min in air.

The thermal behavior of the CBSF glasses was examined by a simultaneous thermal analyzer (Discovery SDT650, TA Instruments, New Castle, USA) using a heating rate of 10 °C min^{-1} to 1200 °C in air. Alumina crucible was employed as the reference material. The test samples were ball-milled fine glass powders. Softening temperature (T_S) measurements for glass were carried out on 6 mm × 5 mm cylindrical glass green samples using a Thermo Mechanical Analysis (TMA 450, TA Instruments, New Castle, USA) at a heating rate of 5 °C min^{-1}. The coefficient of thermal expansion (CTE, ppm/°C) was measured using a Thermo Mechanical Analysis (TMA, TMA 402-F3-Hyperion, NETZSCH, Selb, Germany) under air atmosphere from 25 to 300 °C at a heating rate of 5 °C min^{-1}. The chemical composition analysis of the CBS samples was performed using a Fourier Transformation Infrared Spectrometer (FTIR, INVENIO R & Hyperion 1000, Bruker, Billerica, MA, USA)

scanned from 400 to 1600 cm^{-1} with a resolution of 4 cm^{-1} at room temperature. The phase structure analysis was carried out by an X-ray diffraction (XRD, Bruker D8 Advance, Billerica, MA, USA), in a 2θ range of 20–60° with a step size of 0.02°/s and a CuKα radiation source. The samples used for XRD were the sintered glass-ceramic powders after crushing and grinding. Raman spectroscopy (Jobin Yvon LabRAM HR800, Horiba, Ltd., Kyoto, Japan) was also used to investigate the samples in the wavenumber range of 100–1600 cm^{-1}. The bulk densities of the sintered samples were measured by the Archimedes method using water as media. The microstructure of the sintered samples with polished surfaces was observed by a scanning electron microscope (SEM, Apreo 2 Hivac, Thermo Fisher Scientific Inc., Waltham, MA, USA), and the elemental analysis was carried out with energy dispersive spectroscopy (EDS). Furthermore, the microwave dielectric performance of sintered samples was measured by the shielded cavity method dielectric resonator in the TE011 mode using a network analyzer (Keysight, E5071C ENA, Santa Rosa, CA, USA) at room temperature. The thermal conductivity (λ) of the sintered samples was measured using the Interface Material Thermal Resistance and Heat Conduction System Number Measuring Device (Ruiling LW-9389, Taiwan, China).

3. Results and Discussion

The -XRD patterns of CBS glass-ceramics doped with 0–16 mol% CaF_2 content and sintered at 750 °C and 800 °C were investigated, as presented in Figure 1a–c. The analysis indicates that for the samples of CBSF0 without CaF_2, only a small amount of $CaSiO_3$ (PDF#76-0925) crystals were precipitated at 750 °C. With the addition of CaF_2, the CBSF samples are mainly composed of $CaSiO_3$ (PDF#76-0925) and CaB_2O_4 (PDF#32-0155) crystalline phases. The intensity of $CaSiO_3$ is observed to increase significantly with the increase in CaF_2 content from 0 to 16 mol%, followed by a gradual weakening with a slight shift to the right, while a small amount of CaB_2O_4 phase was precipitated, which suggests that an appropriate amount of CaF_2 can promote the crystal precipitation of $CaSiO_3$. However, with the increase in CaF_2, the high fluorine content causes the crystallization rate of glass to be too fast, resulting in the formation of coarse grains, as well as a great reduction in the intensity of diffraction peaks. As shown in Figure 1b, the results further show that the intensity of $CaSiO_3$ diffraction peaks increases significantly for CBSF0 and CBSF4 during sintering at 800 °C, indicating a greater amount of crystalline phase precipitation at 800 °C than at 750 °C. Figure 1c is a local enlargement of Figure 1b. It can be seen from Figure 1c that the diffraction peak 2θ value of a CBSF sample doped with CaF_2 shifts to the right by about 0.05 degrees, which is ascribed to the smaller ionic radius of F^- ion (1.36 Å) compared to that of O^{2-} ion (1.4 Å). The F^- ion replaces part of O^{2-} ion, and diffuses into the newly formed wollastonite crystals, resulting in the reduced cell parameters of $CaSiO_3$.

The differential scanning calorimetry (DSC) plot of CBSF glass powder with different CaF_2 content is presented in Figure 1d. The exothermic peak observed in the DSC curve corresponds to the occurrence of crystallization during the heating of the glass powder. The analysis reveals that the crystal peaks are concentrated between 839 °C and 727 °C, with an increase in CaF_2 content resulting in a gradual decrease in the starting temperature of glass crystallization (Tx) and the crystallization temperature (Tp), from 810 °C and 839 °C to 705 °C and 727 °C, respectively. This decrease in Tx and Tp is due to the effective reduction in overheating required for crystallization by CaF_2, which promotes crystallization at low temperatures [12–15,20,22].

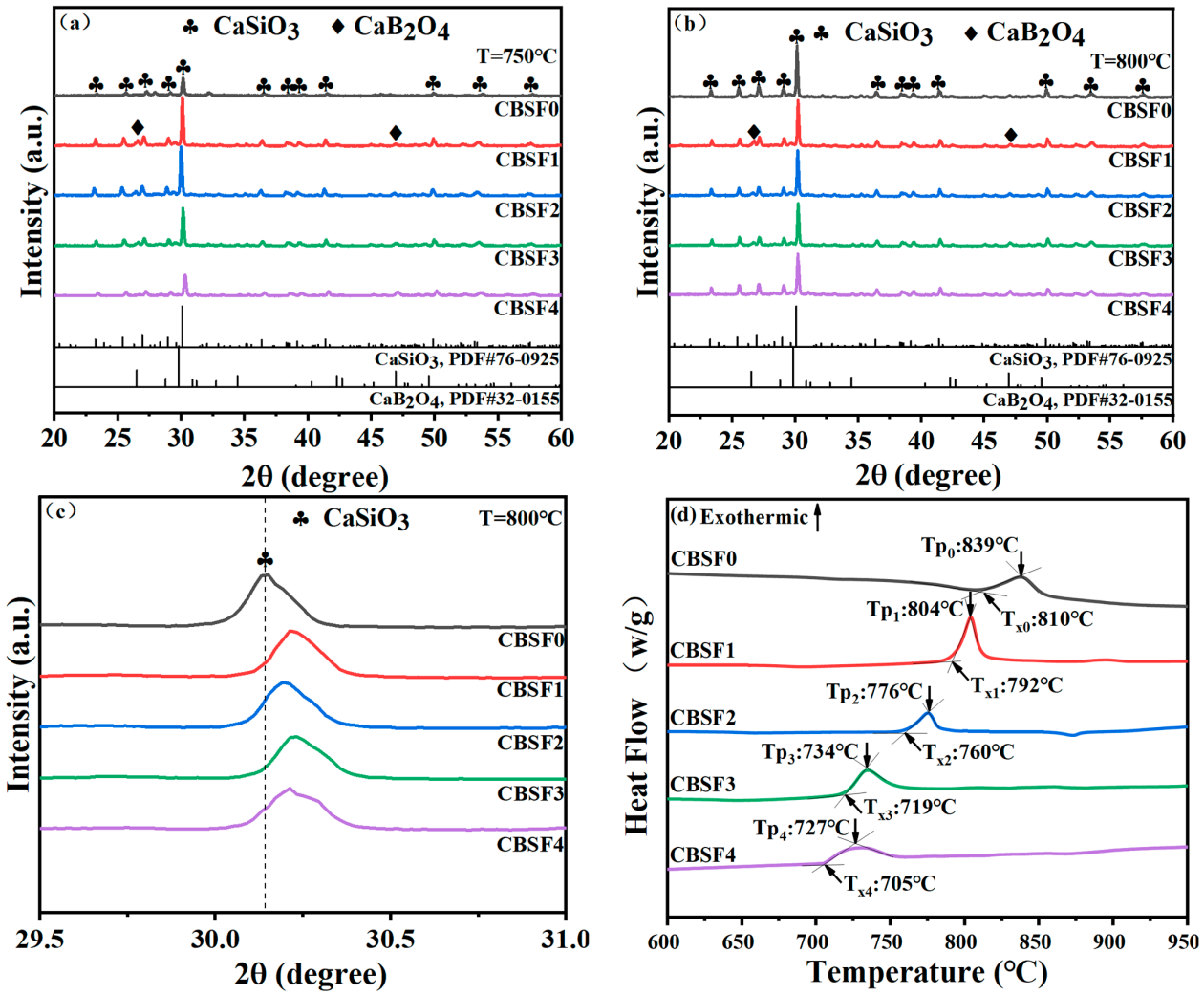

Figure 1. (**a**) XRD patterns of the CBSF glass-ceramics sintered at 750 °C; (**b**,**c**) XRD patterns of the CBSF glass-ceramics sintered at 800 °C; (**d**) DSC curves for the CBSF powder samples.

Figure 2a presents the sintering shrinkage curve of CBSF glass doped with varying CaF_2 contents. The sintering of the glass powder is predominantly governed by viscous flow mass transfer and is closely linked to the viscosity (η) of the glass melt. The softening temperature (Ts) of the glass denotes the temperature at which the glass η is $10^{7.65}$ Pa·s. Prior to the Ts, the glass melt exhibits a high η and a large viscous flow resistance, resulting in contraction of the sample with a flat shape. After the Ts, the glass undergoes softening and rapid deformation due to its self-weight, accompanied by gradual appearance of the liquid phase. The glass powder initiates sintering, with a substantial drop in η and corresponding decrease in viscous flow resistance, leading to a rapid increase in sintering rate. Thereafter, crystal phase precipitation occurs, resulting in an increase in glass melt η and viscous flow resistance, thereby causing the contraction rate to slow or stop. Figure 2b depicts the variation in Ts, maximum shrinkage temperature, and sintering shrinkage rate with CaF_2 doping. The Ts of CBSF glass decreases from 738 °C to 662 °C with an increase in CaF_2 content. The maximum shrinkage temperature is observed to be slightly lower than the crystallization starting temperature, indicating earlier crystallization during the actual sintering process. The sintering shrinkage rate increases from 22% to 24% and subsequently decreases to 16%. Notably, the surface of the CaF_2-doped sample expands beyond a sintering temperature of 825 °C, due to closure of open stomata within the sintering body to form a large, closed stoma under the influence of the internal stress exerted by the large number of liquid phase glass [21–24]. Figure 2b further portrays the

variation in bulk densities of the CBSF with sintering temperature. The CBSF4 sample, sintered at 675 °C, exhibits the highest density of 2.79 g/cm^3, while the CBSF0 sample, sintered at 850 °C, shows the maximum density of 2.75 g/cm^3. The density of CBSF1, CBSF2, CBSF3, and CBSF4 samples increases gradually with sintering temperature, after reaching the maximum value, the density decreases slightly, and the density decreases significantly at around 790 °C. At high sintering temperatures, the enhancement of viscous flow increases the sample density until the maximum density is achieved. However, as the sintering temperature increases, a large number of crystal phases precipitate, resulting in a decrease in sintering density. Furthermore, excessive addition of CaF_2 may produce local internal stress, leading to micro-cracks in the microstructure of glass-ceramic materials and preventing further sintering of ceramics. The results demonstrate that CaF_2 not only lowers the sintering temperature but also prevents ceramics from further sintering by cracking.

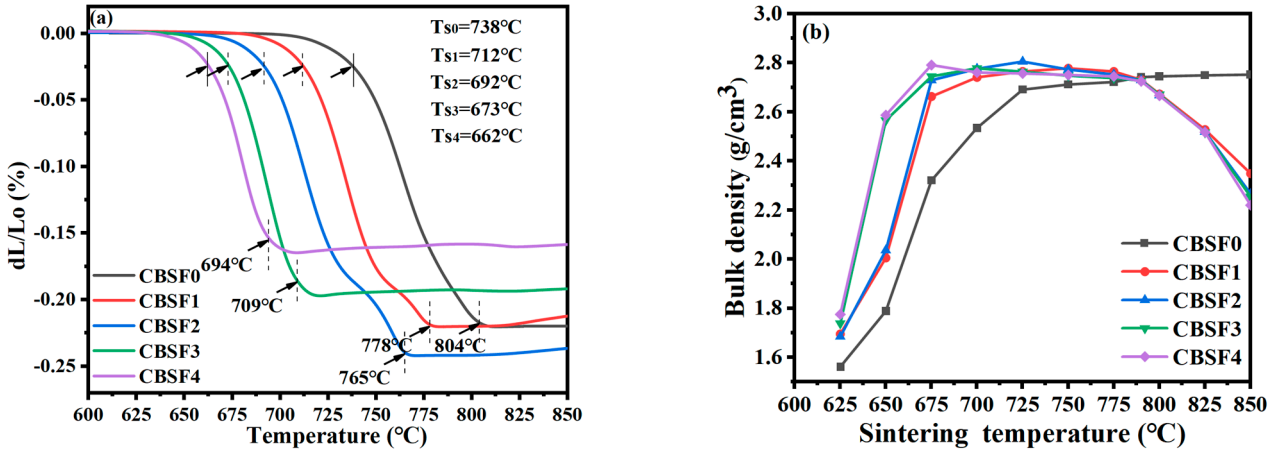

Figure 2. (**a**) The sintering shrinkage profile of CBSF glass-ceramics; (**b**) bulk densities of CBSF glass-ceramics sintered at different temperatures.

The SEM images of CBSF glass-ceramics with varying CaF_2 content sintered at 790 °C are presented in Figure 3a–e. The CBSF1 and CBSF2 samples exhibit better densification with fewer holes on the surface. The EDS results show that the elements Ca, B, and Si were uniformly distributed, while fluorine is enriched, replacing some oxygen ions in the lattice.

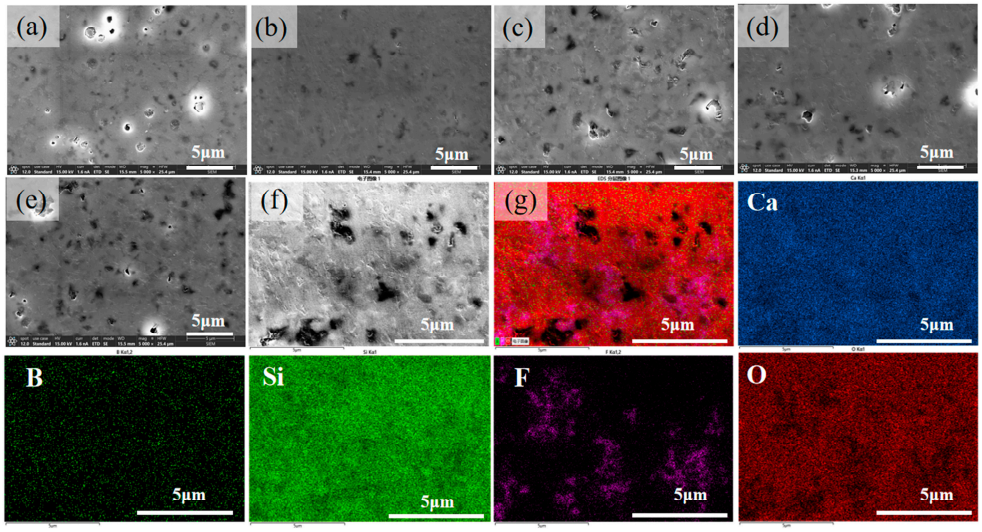

Figure 3. SEM images of the CBSF glass-ceramics: (**a**) CBSF0; (**b**) CBSF1; (**c**) CBSF2; (**d**) CBSF3; (**e**) CBSF4; (**f**,**g**) The EDS mapping results of CBSF2.

The FTIR absorption spectra were used to analyze the bond vibrations, including stretching, bending, and rotating vibrational modes in the molecular structure. Figure 4a illustrates the absorption spectra result of CBSF glass powder samples, with infrared absorption peaks concentrated in four regions: 400–600 cm^{-1}, 600–800 cm^{-1}, 800–1200 cm^{-1}, and 1200–1600 cm^{-1}, corresponding to the Si-O-Si bending, B-O-B bending, [SiO_4] and [BO_4] stretching, and [BO_3] stretching vibrations, respectively [14,25–27]. The addition of CaF_2 with different contents has a significant effect on the CBSF absorption band, as observed by the changes in the intensity of the absorption peaks. The results demonstrate that the addition of CaF_2 alters the structural units of [SiO_4] tetrahedral and [BO_4] tetrahedral, leading to the depolymerization of the O-Si-O bond and the gradual disappearance of large silicate structural units. The Raman spectrum of the CBSF0-CBSF4 glass-ceramics samples sintered at 790 °C and room temperature is presented in Figure 4b, which shows three main sources of Raman peaks: O/F-Ca-O/F bending (<400 cm^{-1}), O-Si-O bending (400–800 cm^{-1}), and Si-O stretching (>800 cm^{-1}) [24]. The addition of CaF_2 results in changes in the anion type and coordination in the Ca-O/F polyhedral, which is reflected by weak Raman peaks at 109, 139, and 1335 cm^{-1} in the CBSF1-CBSF4 samples. The O-Si-O symmetric stretch-bending is observed at ~415, 463, 638, and 735 cm^{-1}, and the Si-O stretching patterns are identified at ~972, 1046, and 1332 cm^{-1}, with the peaks gradually decreasing as CaF_2 content increases, and eventually forming $CaSiO_3$. The Raman spectrum is found to be more sensitive to the local structure compared to XRD analysis, providing information on symmetry, chemical bonds, ion motion, and intermolecular interactions.

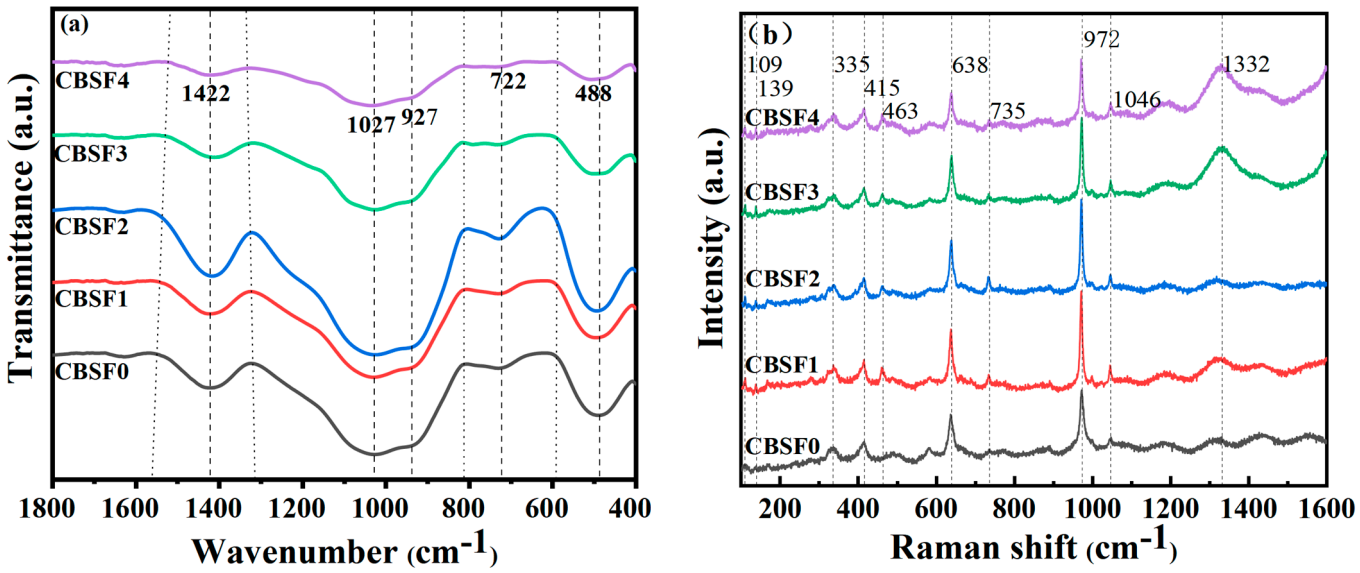

Figure 4. (**a**) FTIR spectra and (**b**) Raman spectra of the CBSF glass-ceramics.

Microwave dielectric properties (ε_r and tanδ) of CBSF samples sintered at different temperatures for 30 min were measured and presented in Figure 5a,b. The findings reveal that the dielectric constant (ε_r) of CBSF glass-ceramics decreases with increasing sintering temperature. In contrast, the dielectric loss (tanδ) of CBSF0 decreases gradually, and CBSF1 and CBSF2 initially decrease and then increase, while CBSF3 and CBSF4 exhibit a gradual increase with increasing sintering temperature. Among all the samples, the CBSF2 glass-ceramic sintered at 790 °C for 30 min demonstrates excellent microwave dielectric properties, with $\varepsilon_r \sim 5.92$ @ 11.4 GHz and tanδ ~ 1.59×10^{-3}. The dielectric properties of the material were primarily determined by the collective contribution of each phase inside. XRD analysis reveals that with an increase in sintering temperature, the precipitation of the $CaSiO_3$ crystalline phase increases, leading to a decrease in ε_r for CBSF glass-ceramics. With the increase in temperature, the tanδ of CBSF0 decreases gradually. This is because the sample porosity in ceramics decreases with the increase in sintering density, which is

conducive to reducing the inconsistency of tanδ of signal transmission energy in ceramics, which is consistent with the sintering density trend of the CBSF0 sample in Figure 2b. The tanδ of CBSF1 and CBSF2 initially decreases and then increases, which may be due to the increase in pores in the ceramics caused by over-burning after the ceramics were further sintered, leading to the deterioration of tanδ [14]. In addition, at the high frequency, tanδ of wollastonite is mainly caused by the thermionic relaxation polarization caused by impurity ions and the conductivity loss of impurity ions, and increases with the increase in temperature [28]. FTIR results indicates that the excessive addition of CaF_2 may have disrupted the network structure of the glass; excess fluorine ions diffused in the $CaSiO_3$ crystalline phase, causing lattice distortion, leading to the tanδ of CBSF3 and CBSF4 samples increasing continuously with the increase in temperature. Furthermore, SEM reveals that the microstructure of the sintered sample is not sufficiently dense, with residual pores, resulting in a similar variation of tanδ.

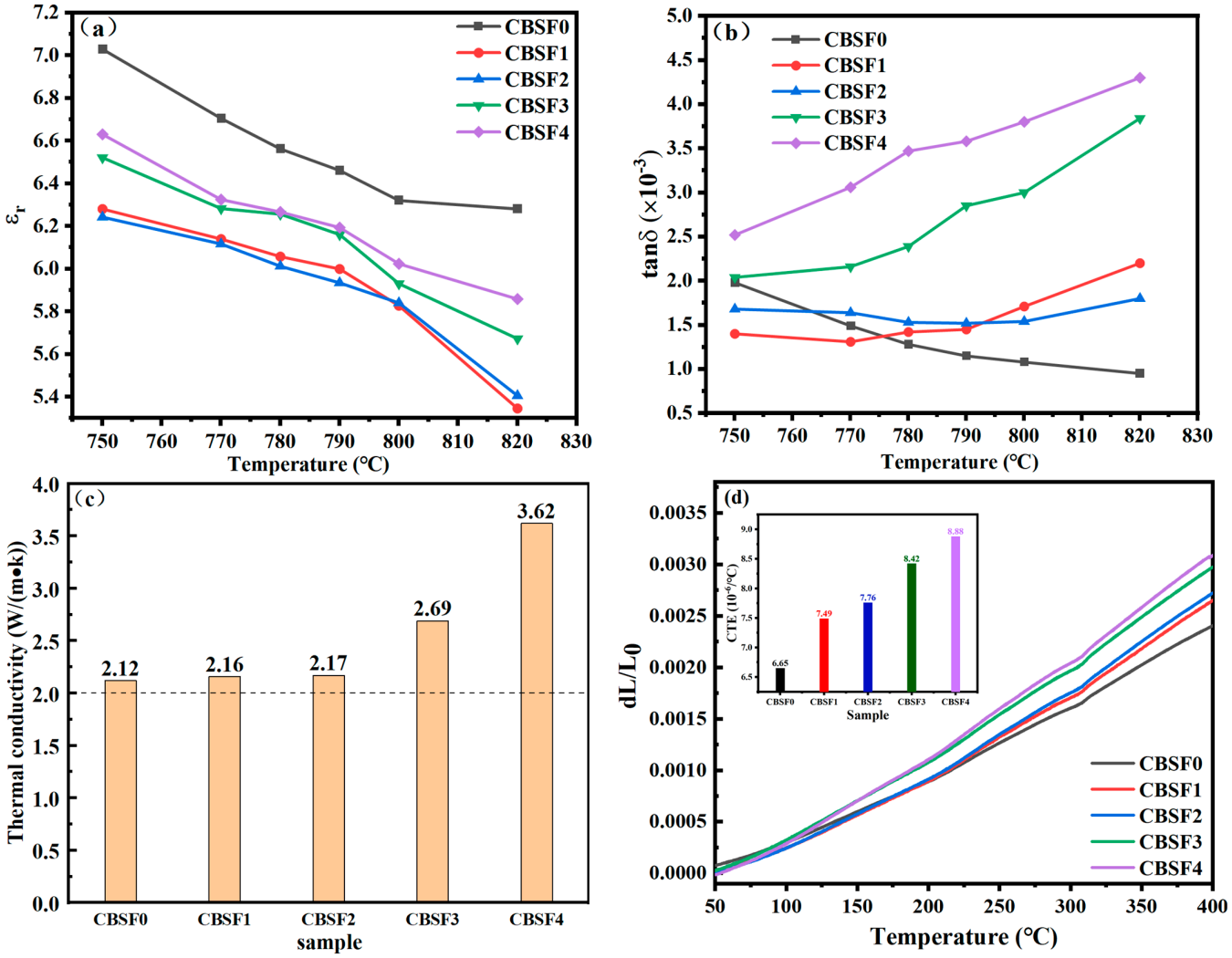

Figure 5. (**a**,**b**) Microwave dielectric properties, (**c**) thermal conductivity, and (**d**) the thermal expansion coefficient of CBSF glass-ceramics.

In Figure 5c, the λ of CBSF glass-ceramics doped with 0–16 wt% CaF_2 sintered at 790 °C is presented. The findings demonstrate that the λ of the CBSF samples increases gradually with an increase in CaF_2 content, with a maximum value of 3.62 W/(m·k) for CBSF4, which is mainly attributed to the partial destruction of the Si-O-Si structure by fluorine ions, decreasing the glass viscosity, leading to liquid phase formation at low temperatures and

promoting the sintering compaction of the ceramic [29,30]. In Figure 5d, the CTE of CBSF glass-ceramics doped with 0–16 wt% CaF_2 sintered at 790 °C is presented, which shows that the linear deformation of glass ceramics increases from room temperature to 400 °C. The CTE value is found to increase from 6.65 × 10^{-6}/°C to 8.88 × 10^{-6}/°C with an increase in CaF_2 content, which is favorable for LTCC applications.

Based on the above results, CaF_2 is proved to be a successful sintering aid for CBS glass-ceramics, significantly reducing its crystallization temperature and viscosity while promoting the precipitation of $CaSiO_3$ crystals. The addition of an appropriate amount of CaF_2 benefits the reduction in ε_r, particularly in the CBSF2 sample doped with 8 mol% CaF_2. The optimal sintering temperature is reduced by 60 °C, from 850 °C to 790 °C, when comparing it to samples without CaF_2 doping (CBSF0). The precipitation temperature of the $CaSiO_3$ crystal decreases from 839 °C to 776 °C, and the crystallization temperature decreases by almost 63 °C. The softening temperature of glass, which is an important index that represents the viscosity of glass, reduced from 738 °C to 692 °C, nearly 46 °C lower. The ε_r is also found to decrease from 6.46 to 5.92 after sintering at 790 °C. However, excessive CaF_2 addition may lead to an increase in the CTE and deterioration of tanδ of CBS glass-ceramics.

Further XRD, SEM, EDS, FTIR, and Raman analyses reveal that with the addition of CaF_2, F^- ions replace some position of O^{2-} ions, resulting in the fracture of Si-O bonds, reduction in [SiO_4] tetrahedrons, [BO_3] triangles, and [BO_4] tetrahedrons, and an enrichment of F^- ions. This ultimately leads to the formation of a broken glass network, damaging its continuity. Additionally, the electrification of the F^- ion differs from that of the O^{2-} ion, and too much addition of F^- ions may generate excess charge, damaging the internal structure and increasing intrinsic loss. At a macro perspective, the presence of microcracks on the sample surface and an increase in porosity can prevent further sintering of CBS glass-ceramics, leading to the deterioration of tanδ and an increase in the CTE.

Based on the requirements of LTCC (low $\varepsilon_r < 6$ and low tanδ < 2 × 10^{-3}), 8 mol% CaF_2 doped CBS glass-ceramics sintered at 790 °C exhibit excellent microwave dielectric properties (ε_r ~ 5.92 @ 11.4 GHz, tanδ ~ 1.59 × 10^{-3}), as well as good thermal properties (CTE ~ 7.76 × 10^{-6}/°C, λ ~ 2.17 W/(m·k)), which are attractive for LTCC applications.

4. Conclusions

In conclusion, the sintering behavior, microstructure, microwave dielectric, and thermal properties of CBSF glass-ceramics were investigated regarding different amounts of CaF_2 and sintering temperatures. The results demonstrated that the addition of CaF_2 significantly affected the sintering behavior, microstructure, and properties of the CBSF glass-ceramics. Excessive CaF_2 addition led to a deterioration in the microwave dielectric properties, while increasing CaF_2 content enhanced the thermal conductivity and thermal expansion coefficient. Furthermore, the sintering temperature also influenced the dielectric properties of the material, with $CaSiO_3$ crystalline phase precipitation increasing with higher sintering temperatures, leading to a decrease in the dielectric constant. Additionally, the microstructure of the CBSF glass-ceramics was not fully densified, resulting in residual pores that influenced the thermal properties of the material. The optimal comprehensive performance was obtained in 8 mol% CaF_2 doped CBS glass-ceramics sintered at 790 °C with CTE of 7.76 × 10^{-6}/°C, λ of 2.17 W/(m·k), ε_r of 5.92 @ 11.4 GHz, and tanδ of 1.59 × 10^{-3}. Overall, the study provides valuable insights into the relationship between the composition, microstructure, and properties of CaF_2 doped CBS glass-ceramics, which can inform the development of novel microwave dielectric materials for LTCC applications.

Author Contributions: Conceptualization, D.W.; methodology, T.Y.; validation, J.Z.; investigation, C.D.; resources, D.W.; writing—original draft preparation, C.D.; writing—review and editing, D.W., H.W. and J.X.; supervision, D.W., H.W. and J.X.; funding acquisition, D.W. All authors have read and agreed to the published version of the manuscript.

Funding: This research was funded by Shenzhen Science and Technology Innovation Committee grant number JCYJ20220531095802005.

Data Availability Statement: Not applicable.

Acknowledgments: The authors gratefully acknowledge the financial support from Shenzhen Science and Technology Innovation Committee (JCYJ20220531095802005).

Conflicts of Interest: The authors declare no conflict of interest.

References

1. Wei, A.; Wang, G.; Liu, X. *Low-Temperature Co-Fired Ceramic Materials and Applications*; Springer: Singapore, 2018.
2. Imanaka, Y. *Multilayered Low Temperature Cofired Ceramics (LTCC) Technology*; Springer Science + Business Media, Inc.: Berlin/Heidelberg, Germany, 2005; pp. 2–5.
3. Zhang, M.; Li, J.; Li, X. LTCC Substrates for Microwave Applications. *Micromachines* **2021**, *12*, 526.
4. Li, H.; Li, H.; Li, S. Research on Preparation and Properties of High-Performance LTCC Materials. *Materials* **2021**, *14*, 74.
5. Xu, C.; Chen, J.; Fang, Z. Development of LTCC Technology and Applications. *Int. J. Appl. Ceram. Technol.* **2016**, *13*, 1036–1047.
6. Lin, Z.; Li, M.; He, J.; Li, M.; Wang, G.; Li, Y.; Zeng, Y.; Han, J.; Liu, J. Effect of Ta_2O_5 addition on the structure, crystallization mechanism, and properties of $CaO–B_2O_3–SiO_2$ glasses for LTCC applications. *Ceram. Int.* **2023**, *49*, 4872–4880. [CrossRef]
7. Hsiang, H.-I.; Chen, C.-C.; Yang, S.-Y. Structure, crystallization, and dielectric properties of the Al_2O_3 filled $CaO–B_2O_3–SiO_2–Al_2O_3$ glass composites for LTCC applications. *Jpn. J. Appl. Phys.* **2019**, *58*, 91010. [CrossRef]
8. He, D.; Zhong, H.; Gao, C. Effect of TiO_2 doping on crystallization, microstructure and dielectric properties of CBS glass-ceramics. *J. Alloys Compd.* **2019**, *799*, 50–58. [CrossRef]
9. Zhu, H.; Fu, R.; Agathopoulos, S.; Fang, J.; Li, G.; He, Q. Crystallization behaviour and properties of BaO-CaO-B_2O_3-SiO_2 glasses and glass-ceramics for LTCC applications. *Ceram. Int.* **2018**, *44*, 10147–10153. [CrossRef]
10. Xiang, Y.; Han, J.; Lai, Y.; Li, S.; Wu, S.; Xu, Y.; Zeng, Y.; Zhou, L.; Huang, Z. Glass structure, phase transformation and microwave dielectric properties of $CaO–B_2O_3–SiO_2$ glass–ceramics with addition of La_2O_3. *J. Mater. Sci. Mater. Electron.* **2017**, *28*, 9911–9918. [CrossRef]
11. Han, J.; Xiang, Y.; Yao, Z.; Zeng, Y.; Bai, P.; Jiang, Y.; Chen, W. Glass structure, crystallization kinetics and dielectric properties of CeO_2-added $CaO–B_2O_3–SiO_2$ glass system. *J. Mater. Sci. Mater. Electron.* **2019**, *30*, 5902–5910. [CrossRef]
12. He, D.; Zhong, H.; Gao, C. Characteristics and dielectric properties of ZrO_2-doped calcium borosilicate glass-ceramics. *Mater. Res. Bull.* **2020**, *123*, 110703. [CrossRef]
13. Yang, C.; Li, J.; Lu, Y.; Shan, Y.; Xian, Q.; Zhou, H. Sintering behaviors, microstructures and dielectric properties of CaO-B_2O_3-SiO_2 glass ceramic for LTCC application with various network modifiers content. *J. Mater. Sci. Mater. Electron.* **2021**, *32*, 26655–26665. [CrossRef]
14. Zhu, X.; Kong, F.; Ma, X. Effects of LiF on sintering behavior and properties of CaO-B_2O_3-SiO_2 dielectric ceramics obtained by solid-state reaction. *Ceram. Int.* **2018**, *44*, 20006–20011. [CrossRef]
15. Pei, F.; Zhu, G.; Li, P.; Guo, H.; Yang, P. Effects of CaF_2 on the sintering and crystallisation of $CaO–MgO–Al_2O_3–SiO_2$ glass-ceramics. *Ceram. Int.* **2020**, *46*, 17825–17835. [CrossRef]
16. Si, W.; Zhang, L.-N. Crystallization kinetics of wollastonite glass ceramics doped calcium fluoride. *Chin. J. Nonferrous Met.* **2020**, *31*, 1020–1026.
17. Si, W.; Ding, C.; Zhang, W.-Y. Effect of calcium fluoride on properties of glass ceramics prepared by reaction crystallization of sodium-calcium glass. *J. Chin. Ceram. Soc.* **2012**, *40*, 703–707.
18. Zhao, Y.-C.; Xiao, H.-N.; Tan, W. Effect of CaF_2 addition amount on crystallization process and material properties of glass ceramics. *J. Chin. Ceram. Soc.* **2002**, *9*, 33–36.
19. Si, W. Effect of fluoride on properties of wollastonite glass ceramics. *Bull. Chin. Ceram. Soc.* **2020**, *39*, 2281–2284.
20. Qin, J.; Liu, Z.; Ma, M.; Li, Y. Crystal structure, lattice vibration and microwave dielectric properties of 3CaO·2SiO2·xCaF2 ($0 \leq x \leq 1.5$) ceramics. *Ceram. Int.* **2022**, *48*, 14371–14377. [CrossRef]
21. Dong, C.; Yan, T.; Xu, J.; Li, Z.; Sun, R.; Wang, D. The effects of B_2O_3 content and Ca/Si ratio on the densification behavior and microwave dielectric properties of the CaO-B_2O_3-SiO_2 glass-ceramics for LTCC application. In Proceedings of the 2022 23rd International Conference on Electronic Packaging Technology (ICEPT), Dalian, China, 10–13 August 2022; pp. 1–3.
22. Sujirote, K.; Rawlings, R.D.; Rogers, P.S. Effect of fluoride on sinterability of a silicate glass powder. *J. Eur. Ceram. Soc.* **1998**, *18*, 1325–1330. [CrossRef]
23. Chiang, C.-C.; Wang, S.-F.; Wang, Y.-R.; Hsu, Y.-F. Characterizations of $CaO–B_2O_3–SiO_2$ glass–ceramics: Thermal and electrical properties. *J. Alloys Compd.* **2008**, *461*, 612–616. [CrossRef]
24. Wang, S.-F.; Wang, Y.-R.; Hsu, Y.-F.; Chiang, C.-C. Densification and microwave dielectric behaviors of $CaO–B_2O_3–SiO_2$ glass-ceramics prepared from a binary glass composite. *J. Alloys Compd.* **2010**, *498*, 211–216. [CrossRef]
25. Yan, T.; Zhang, W.; Mao, H.; Chen, X.; Bai, S. The effect of CaO/SiO_2 and B_2O_3 on the sintering contraction behaviors of CaO-B_2O_3-SiO_2 glass-ceramics. *Int. J. Mod. Phys. B* **2019**, *33*, 1950070. [CrossRef]

26. Zhang, W.; Chen, Z.; Wang, F.; Chen, X.; Mao, H. Comprehensive effects of La/B ratio and CaO additive on the efficiency of lanthanum borate glass–ceramics as sintering aids for LTCC application. *J. Mater. Sci. Mater. Electron.* **2021**, *32*, 24369–24380. [CrossRef]
27. Kim, G.H.; Sohn, I. Effect of CaF_2, B_2O_3 and the CaO/SiO_2 mass ratio on the viscosity and structure of B_2O_3-containing calcium-silicate-based melts. *J. Am. Ceram. Soc.* **2019**, *102*, 6575–6590. [CrossRef]
28. He, M.; Mu, D.; Huang, J. *Modification and Mechanism of Wollastonite Based LTCC Ceramic Substrate Materials*; Science Press: Beijing, China, 2014; pp. 89–92.
29. Wang, S.-F.; Lai, B.-C.; Hsu, Y.-F.; Lu, C.-A. Dielectric properties of $CaO–B_2O_3–SiO_2$ glass-ceramic systems in the millimeter-wave frequency range of 20–60 GHz. *Ceram. Int.* **2021**, *47*, 22627–22635. [CrossRef]
30. Wang, S.-F.; Lai, B.-C.; Hsu, Y.-F.; Lu, C.-A. Physical and structural characteristics of sol–gel derived $CaO–B_2O_3–SiO_2$ glass-ceramics and their dielectric properties in the 5G millimeter-wave bands. *Ceram. Int.* **2022**, *48*, 9030–9037. [CrossRef]